24th COBEM - 2017

24th ABCM International Congress of Mechanical Engineering
December 3-8, 2017, Curitiba, PR, Brazil

COBEM-2017- 0836
MATHEMATICAL MODEL OF A HEAT EXCHANGER OPERATING WITH EMISSIONS FROM A THERMAL TREATMENT OF MUNICIPAL SOLID WASTE

Matias Nicolas Muñoz
Universidade Federal do Paraná, Núcleo de Pesquisa e Desenvolvimento de Energia Autossustentável, Francisco H dos Santos, S/N Centro Politécnico, Setor de Tecnologia - Jardim das Americas, Curitiba - PR, 81531-990, Brazil.
Centro de Estudios de Energía para el Desarrollo - CEED, Facultad de Ingeniería, Oberá - Misiones, 3360, Argentina.
matiasmunuoz@gmail.com
José Coelho Viriato Vargas
Universidade Federal do Paraná, Departamento de Engenharia Mecânica, Francisco H dos Santos, S/N Centro Politécnico, Setor de Tecnologia - Jardim das Americas, Curitiba - PR, 81531-990, Brazil.
vargasjvcv2@gmail.com
Wellington Balmant
Universidade Federal do Paraná, Núcleo de Pesquisa e Desenvolvimento de Energia Autossustentável, Francisco H dos Santos, S/N Centro Politécnico, Setor de Tecnologia - Jardim das Americas, Curitiba - PR, 81531-990, Brazil.
wbalmant@gmail.com

Abstract. *In this work, we consider the basic thermodynamic problem of extracting the greatest amount of energy from a hot exhaust flow. The objective is thermodynamical to optimize the system, locating the optimal capacity rate and the out temperature of the cold stream. Thus, a non-dimensional mathematical model of a heat exchanger is presented in steady state with phase changes of the cold current. For the model, we use the basic principle of classical thermodynamics and the concept of heat transfer, obtaining nonlinear equations to be constructed by computer code. The temperature entering the water, considered for this analysis, corresponds to* $T_1=334$ *K enters as condensate and boils at* $T_b=444$ *K. The pressure that is exposed to the current of water is 8 bar. However, the inlet temperature of the hot gas is* $T_H=1,072$ *K. We have found that the optimal capacity rate of the cold current is* $M_{opt}=0.18$*. If M varies the temperature distributions changes and the second law, efficiency exhibits a maximum at value* M_{opt}*. It means that any stream can be matched optimally, such that most of the exergy carried by the hot stream is captured by the cold stream.*

Keywords: *Mathematical modelling, thermodynamic optimization, urban solid waste, heat exchanger*

1. INTRODUCTION

In our day-to-day, the consumption of diverse resource is a basic principle of humanity; this uncontrolled consumption generates large amounts of waste, which must be treated safely, efficiently and effectively. The management of large quantities of waste is a challenge for society; it is for this MSW (municipal solid waste) continues to be one of the priorities of human communities in the 21st century. (Albores et al., 2016).

Global generation of solid urban waste is expected to increase to 27 million tons by 2050 due to population growth, urbanization and socio-economic development in low-and middle-income countries, (Beede and Bloom, 1995). According to the Organization for Economic Co-operation and Development (OECD), annual production of MSW is estimated at 1.9 million tons, and it is believed that approximately 30% of this amount will not be collected by municipal services. MSW collected, 70% are taken to landfills, 19% will be reused or recycled and only 11 % will be used in facilities to recover energy.

Incineration is one of the most widely used technologies in the world (Liu and Liu, 2005) about 181 million tons of MSW are burned annually in more than 600 WTE (waste to energy) facilities worldwide. MSW heat treatment avoids the aqueous and gaseous contamination associated with the landfill and provides a source of renewable energy; having as profit a reduction of up to 75% by weight and 90% by volume of waste. As a secondary benefit heat is obtained for the generation of energy (electric and thermal), it is also common the cogeneration, that is the additional recovery of heat from the steam used. In analyzing the incineration process, gases exiting the combustion chamber carry heat, which are used in energy recovery equipment such as a heat exchanger, where the transfer of heat between the hot gases and a cold-water flow obtains energy. Subsequently, the recovered energy is used to move a turbine that is coupled to a generator to produce electrical energy. (Lombardi et al., 2015).

In this study, we focus on the energy recovery process that is obtained from the heat treatment of MSW specifically in the heat exchanger used to extract heat from a hot gas stream (flue gas) to heat a stream of cold water.

We consider a basic situation of thermodynamics: how to extract the maximum of the mechanical power from a hot exhaust flow. The problem is observed in Figure 1, where ṁ is the mass flow rate and the initial T_H temperature of the gases from the thermal waste treatment. (Bejan and Errera, 1998). This fluid behaves as an ideal gas with constant c_p, the temperature T_H of the hot current will decrease as it exchanges heat with the cold current. Therefore, it is sought to maximize the output power $\dot{W}$ or minimize the total rate of entropy generation of the heat exchanger.

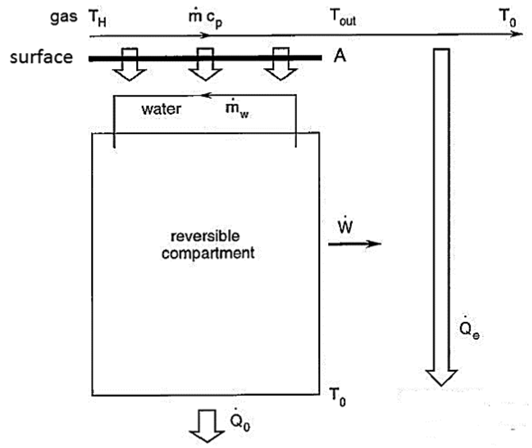

Figure 1. The extraction of hot output power flow.

The heat is transported through the gas stream and transferred to the working fluid (water), the latter being the one that takes the most time to complete the power cycle. The mass flow of this second stream, $\dot{m}_w$, is not fixed. The heat transfer between both streams occurs through a heat transfer surface *A*, which is fixed. The problem of thermodynamic optimization is equivalent to finding the best relation between the mass flow rate $\dot{m}$ and the mass flow rate of the water stream $\dot{m}_w$. In this problem, we have to consider some issues. First, the water stream may experience a change of phase (vaporization) over an intermediate section of the heat exchanger, where the water temperature remains constant. The second state is imposed by the heat transfer surface *A*. In the cold side, the heat transfer surface is actually a succession of three sections: the surface A_s with superheat stream, the surface A_b over which the stream boils and the surface A_w where the liquid water is heated to the boiling point (Vargas et al., 2001). The surface *A* is defined by:

$$A = A_s + A_b + A_w \tag{1}$$

In order to have a clearer understanding of the problem is presented in Figure 2 schematically the temperature distribution occurring within the heat exchanger

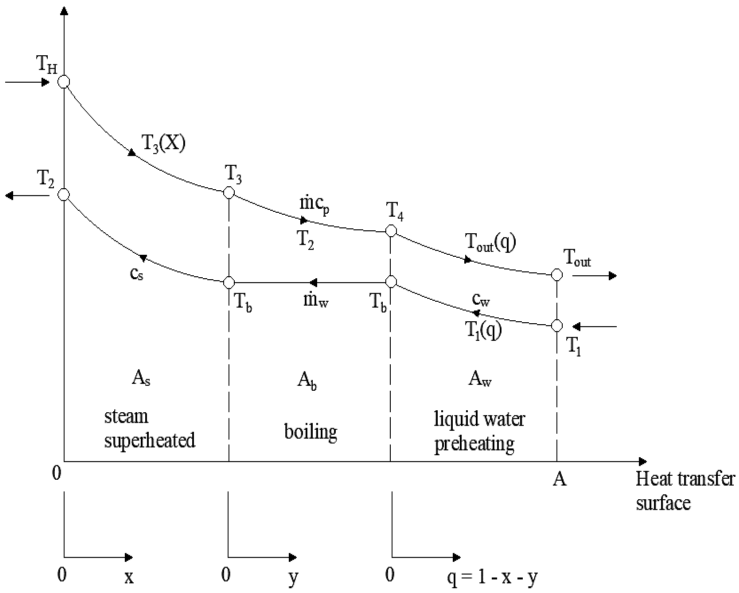

Figure 2. Temperature distribution diagram of the heat exchanger.

We have to consider that the cold side has a coefficient of heat transfer for each section, i.e., U_w over the A_w section, U_b over the boiling section A_b and U_s over the superheating section A_s.

The third complication of the problem of thermodynamic optimization is imposed by flow giving that is not defined, so we must find the optimum ratio to obtain the best possible heat exchanger performance. Figure 2 shows the temperature distribution of the gases and the working fluid where the three sections that the cold fluid undergoes in the heat exchanger are observed.

2. HEAT TRANSFER ANALYSIS

The method of entropy generation minimization combines thermodynamics with the heat transfer. The heat transfer analysis is to determine a relationship between the rate of entropy generation, the physical parameters and the limitations of the modeling system.

The hot gas flow and the water flow work counter currently, we assume that the water enters as a subcooled liquid (T_1, P_1) over time, the water stream boils and overheats before exiting the heat exchanger with a condition (T_2, P_2). This situation is to observe. This situation can be seen in Figure 2, where the cold side is considered as three subsequent heat exchangers. (Moran et al., 2011).

The heat transfer of each heat exchanger is described by the classical effectiveness NTU relationships. The method is used to determine the final temperatures of the working fluids when having a heat exchanger or if the heat exchange surface is known. It is based on the determination of two-dimensional numbers, and by means of a graph is determined the third number that allows the calculation of the temperature of exit. (Bejan, 1993). First dimensionless number is N:

$$N = \frac{U \cdot A}{C_{low}} \tag{2}$$

Where, U global heat transfer coefficient, A exchange area, c_{low} lower calorific capacity. Another dimensionless number is the capacity coefficient:

$$C_r = \frac{C_{low}}{C_{high}} = \frac{\Delta T_{low}}{\Delta T_{high}} \tag{3}$$

where ΔT is the thermal difference between the inlet and outlet of each fluid.

With the two dimensionless numbers, one obtains the graph corresponding to each heat exchanger. Value of the exchanger effectiveness is defined as the ratio of heat absorbed by the fluid with lowest heat capacity to maximum value that could be changed:

$$\varepsilon = \frac{\text{Heat exchanged by the fluid } C_{low}}{\text{Maximum heat exchanged}} = \frac{\Delta T_{low}}{T_{h,in} - T_{c,out}} \tag{4}$$

where, $T_{h,in}$ is the hot fluid inlet temperature and $T_{c,out}$ the cold fluid inlet temperature. Substituting the terms in Eq. (4) is obtained:

$$\varepsilon_s = \frac{1-\exp\left[-N_s\left(1-C_r\right)\right]}{1-C_r\exp\left[-N_s\left(1-C_r\right)\right]} \tag{5}$$

Proceeding the analysis of the heat exchanger, starting from left to right in Figure 2:

2.1 *Section Superheater* ($0 < X < X_f$)

In this section, the effectiveness is: $\varepsilon_s = \varepsilon_s(x)$, for $\mu < 1$. The size of the heat exchanger is defined as:

$$N_s = \frac{U_s xA}{\dot{m}_w c_s}\frac{\dot{m}c_p}{\dot{m}c_p} = \frac{xN}{\mu} \tag{6}$$

The efficiency for this part of the exchanger is defined as follows:

$$\varepsilon_s = \frac{\dot{m}_w c_s (T_2 - T_2(x))}{\dot{m}_w c_s (T_H - T_2(x))} \tag{7}$$

isolating the temperature $T_2(x)$ from Eq. (7):

$$T_2(x) = \frac{\lfloor T_2 - \varepsilon_s(x) T_H \rfloor}{1 - \varepsilon_s(x)} \tag{8}$$

Performing the analysis for the hot side, the efficiency is presented as follows:

$$\varepsilon_s = \frac{\dot{m} c_p (T_H - T_3(x))}{\dot{m}_w c_s (T_H - T_2(x))} \tag{9}$$

isolating the temperature $T_3(x)$ from Eq. (9):

$$T_3(x) = T_H - \mu\varepsilon_s (T_H - T_2(x)) \tag{10}$$

Considering that the working fluid (water) has the greatest capacity, therefore, the size of the heat exchanger is defined as follows:

$$N_s = \frac{U_s x A}{\dot{m} c_p} \frac{\dot{m} c_p}{\dot{m} c_p} = xN \tag{11}$$

where efficacy is presented by:

$$\varepsilon_s = \frac{\dot{m}_w c_s (T_2 - T_2(x))}{\dot{m} c_p (T_H - T_2(x))} \tag{12}$$

isolating the temperature $T_2(x)$ from Eq. (12):

$$T_2(x) = \frac{T_2 - \frac{\varepsilon_s}{\mu} T_H}{1 - \varepsilon_s / \mu} \tag{13}$$

The temperature $T_3(x)$ is represented by:

$$T_3(x) = T_H - \varepsilon_s (T_H - T_2(x)) \tag{14}$$

2.2 *Section Boiling* ($0 < Y < Y_f$)

In this section the temperature on the cold side is uniform, T_b. The size of the heat exchanger is defined as follows:

$$N_b = \frac{U_b y A}{\dot{m} c_p} \frac{U_s}{U_s} = yN \frac{U_b}{U_s} \tag{15}$$

the efficiency of this part of the exchanger is defined by the following expression:

$$\varepsilon_b(y) = 1 - \exp(-N_b) \tag{16}$$

replacing corresponding terms and isolating the temperature T_4 from Eq. (16):

$$T_4(y) = T_3 - \varepsilon_b(y) \bullet (T_3 - T_b) \quad (17)$$

2.3 *Section Liquid* ($0 < q < q_f$)

For $\mu' = \dfrac{\dot{m}_w c_w}{\dot{m} c_p} < 1$, where c_w is specific heat of liquid water. The size of the heat exchanger is defined as follows:

$$N_w = \frac{U_w (1 - x - y) A}{\dot{m} c_p} \frac{U_s}{U_s} = (1 - x - y) N \frac{U_w}{U_s} \quad (18)$$

The efficiency for this part of the exchanger is defined:

$$\varepsilon_w = \frac{\dot{m}_w c_w (T_b - T_1(q))}{\dot{m} c_p (T_4 - T_1(q))} \quad (19)$$

solving Eq. (19), the intermediate temperature is obtained $T_1(q)$:

$$T_1(q) = \frac{\lfloor T_b - \varepsilon_w T_4 \rfloor}{(1 - \varepsilon_w(q))} \quad (20)$$

for $\mu' > 1$, liquid water with a higher rate of capacity than gas

$$T_1(q) = \frac{T_b - \dfrac{\varepsilon_w}{\mu'} T_4}{1 - \varepsilon_w / \mu'} \quad (21)$$

In summary, the heat exchanger is described by ten equations: three effectiveness-NTU equations [(7), (16) and (19)], seven equations containing the intermediate temperatures of the three sections [(8), (10), (13), (14), (17), (20) and (21)].
The system of ten equations we add the total surface constraint (1), which now reads:

$$N = \mu N_s + \frac{U_s}{U_b} N_b + \mu' \frac{U_s}{U_w} N_w \rightarrow (\mu < 1, \mu' < 1) \quad (23a)$$

$$N = \mu N_s + \frac{U_s}{U_b} N_b + \mu' \frac{U_s}{U_w} N_w \rightarrow (\mu < 1, \mu' > 1) \quad (23b)$$

In this case, it is convenient to apply to Eq. (23) the constraints, introducing the fractions of area presented in the following expressions:

$$x = \frac{A_s}{A}; \quad y = \frac{A_b}{A}; \quad 1 - x - y = \frac{A_w}{A} \quad (24)$$

wit is necessary to determine the derivatives of the equations for heat transfer in each section. For this, we analyze each section inside the heat exchanger

I. Section Superheated. In the case $C_r = \mu$:

$$\frac{T_2 - T_b}{T_4 - T_b} = \varepsilon_s = \frac{1 - \exp[\frac{-xN}{\mu}(1 - \mu)]}{1 - \mu \exp[\frac{-xN}{\mu}(1 - \mu)]} \quad (25)$$

isolating the incognita *x* (area) from Eq. (25) gives the following expression:

$$x = \frac{-\mu \ln(\frac{T_2 - T_b}{T_4 - T_b})}{N(1-\mu)} = f_1(T_2) \tag{26}$$

II. Section Boiling.

$$\frac{T_3 - T_4}{T_3 - T_4} = \varepsilon_b = 1 - \exp(-yN\frac{U_b}{U_s}) \tag{27}$$

performing energy balance for the boiling section is represented by:

$$\dot{m}c_p(T_3 - T_4) = \dot{m}_w hfg(T_b) \tag{28}$$

where, h_{fg} specific latent heat is

$$T_3 - T_4 = \frac{\dot{m}_w c_s hfg(T_b)}{\dot{m}c_p c_s T_0} \tag{29}$$

matching Eqs. (27) and (29) gives expression for the area *y*:

$$y = -\frac{1}{N\frac{U_b}{U_s}} \ln \left(1 - \frac{\mu \ hfg \ T_b}{c_s T_0 (T_3 - T_b)}\right) = f_2(T_2) \tag{30}$$

III. Section Liquid.

$$\frac{(T_b - T_1)}{(T_4 - T_1)} = \varepsilon_w = \frac{1 - \exp[-N_w(1-\mu')]}{1 - \mu'\exp[-N_w(1-\mu')]} \tag{31}$$

isolating the incognita *(1-x-y)* (area) from Eq. (31) gives following expression:

$$(1 - x - y) = \frac{-\mu' \ln\left[\frac{\frac{(T_b - T_1)}{(T_4 - T_1)} - 1}{\frac{(T_b - T_1)}{(T_4 - T_1)}\mu' - 1}\right]}{\frac{U_w}{U_s}N(1-\mu')} = f_3(T_2) \tag{32}$$

an energy balance determines the exhaust gas temperature T_{out} of the heat exchanger is represented by:

$$\dot{m}c_p(T_4 - T_{out}) = \dot{m}_w c_w (T_b - T_1) \tag{33}$$

isolating T_{out} from Eq. (33) gives following expression:

$$T_{out} = T_4 - \mu'(T_b - T_1) \tag{34}$$

2.4 Entropy analysis

There are many ways to perform thermodynamic optimization. Consider the system shown in Figure 1, which contains all the components located at temperatures above T_0, plus the external course followed by $\dot{m}$ as it is hurled into the ambient. The heat transfer that occurs between the external environment and the heat exchanger is described by

$\dot{Q}_1 = \dot{m}(h_{out} - h_0)$, the first and second law for the operation of the steady state heat exchanger, according to. (Manjunath and Kaushik, 2014) are represented by the following expressions:

$$\dot{W} = \dot{m}(h_H - h_0) - \dot{Q}_0 - \dot{Q}_1 \tag{35}$$

$$\dot{S}_{gen} = \frac{\dot{Q}_0 + \dot{Q}_1}{T_0} + \dot{m}(s_0 - s_H) \geq 0 \tag{36}$$

by eliminating $(\dot{Q}_0 - \dot{Q}_1)$ of Eq. (34) and (35):

$$\dot{W} = \dot{m}_w e_{x,H} - T_0 \dot{S}_{gen} \tag{36}$$

In Eq. (36) allows us to observe that the output power is equal to the net flow of exergy in the reversible compartment shown in Figure 1, where $T_0\dot{S}_{gen}$ represents the destroyed exergy and $e_{x,H}$ is the initial specific flow exergy of the hot gas, $e_{x,H}=(h_H - T_0 s_H) - (h_0 - T_0 s_0)$. The final flow exergy of the $\dot{m}$ stream is zero, because at that state $\dot{m}$ reaches thermomechanical equilibrium with the ambient. To calculate $T_0\dot{S}_{gen}$, write the first law and the second law, and eliminate $\dot{Q}_1$ according to (Bejan, 1996):

$$T_0 \dot{S}_{gen} = \dot{m} e_{x,H} - \dot{m}_w (e_{x,2} - e_{x,1}) \tag{37}$$

In Eq. (37) shows, that exergy is the difference between the exergy introduced by the hot gas and the exergy collected by the stream of water. Eliminating $T_0\dot{S}_{gen}$ between Eqs. (36) and (37) obtaining the following expression:

$$\dot{W} = \dot{m}_w (e_{x,2} - e_{x,1}) \tag{38}$$

indicates that the output power is equal to the net exergy flow of the system shown in Figure. 1.

Therefore, the proper dimensionless measure of the thermodynamic optimum is the maximum reached by the second law efficiency. (Bejan, 1996).

$$\eta_{II} = \frac{W}{\dot{m} \quad e_{x,H}} = \frac{\dot{m}_w (e_{x,2} - e_{x,1})}{\dot{m} \quad e_{x,H}} \tag{39}$$

where $e_x = T_0 s$ can be developed into by Eq. (40), in these equations the temperatures are dimensionless by the ratio $\tau_i = T_i/T_0$.

$$\eta_{II} = \frac{\mu(a+b)}{\tau_H - 1 - \ln \tau_H} \tag{40}$$

where, *a* and *b* are described according to (Bruel et al., 2016) as follows:

$$a = \tau_2 - \tau_b - \ln \frac{\tau_2}{\tau_b} \tag{41}$$

$$b = \frac{h_{fg}}{\bar{c}_s T_0}(1 - \frac{1}{\tau_b}) + \frac{c_w}{\bar{c}_s}(\tau_b - \tau_1 - \ln \frac{\tau_b}{\tau_1}) \tag{42}$$

The specific heat of liquid water on tabulated date (Moran et al., 2011), $c_w = c_w(T_b)$ and the specific heat at constant pressure of steam was taken as the average of the tabulated values $\bar{c}_s = 1/2(c_s(T_2) + c_s(T_b))$.

3. SOLUTION NUMERICAL METHOD

In this problem, we have ten unknown parameters these are: x, y, $(1\text{-}x\text{-}y)$, τ_3, τ_4, τ_{out}, τ_2, ϵ_w, ϵ_b and ϵ_s for Eqs (23) to (33). The solution to the system of ten equations for a given set of parameters (M, N, τ_H, τ_b, τ_1, U_b/U_s, U_w/U_s) is obtained by combining Eqs. (26), (30) and (32) delivered $x=f_1(\tau_2)$, $y=f_2(\tau_2)$ and $(1\text{-}x\text{-}y)=f_3(\tau_2)$, using the total surface constant given by Eq. (43) to build the following equations to be solved for T_2.

$$F(\tau_2) = f_3(\tau_2) - \lfloor 1 - f_1(\tau_2) - f_2(\tau_2) \rfloor = 0 \tag{43}$$

Once τ_2 is found, the other unknowns for any specific time interval of the quasi steady for simulation are obtained directly by the model. The maximization of η_{II} was executed using a FORTRAN® code based on combined secant, Newton-Raphson and bisection methods. (Vargas and Araki, 2016). The tolerance $|F(\tau_2)| \leq 10^{-6}$ was imposed in order to achieve convergence in all solutions. The M range for water on cold side was $0.01 \leq M \leq 0.5$. The chosen discretization was the coarsest set for which the optimal M value did not change as the sets became finer, while the relative error was maintained below 1% in all the cases.

4. RESULTS AND DISCUSSIONS

Figure 3a-c shows the temperature distribution within the heat exchanger, when the water and gas stream flows through surface A. The results were obtained assuming that the overall coefficient of heat transfer is equal in the three sections of the exchanger $U_s = U_b = U_w$. The temperatures adopted, for initial simulation, for the water flow at 8 bar, enter the heat exchanger at T_1 = 334 K and boils at T_b = 444 K. The input temperature of the hot gas is T_H = 1,072 K, and we consider the ambient temperature at T_0 = 298 K.

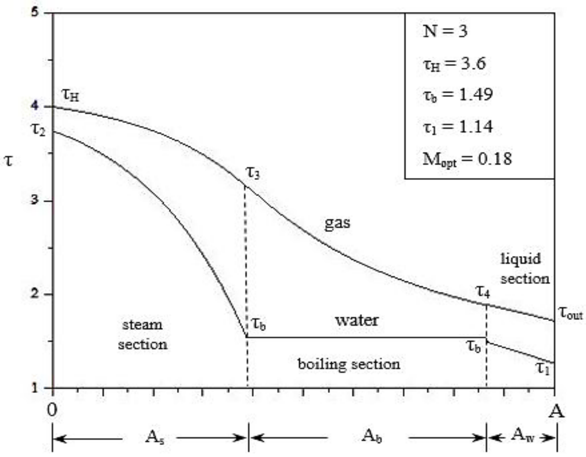

(a)

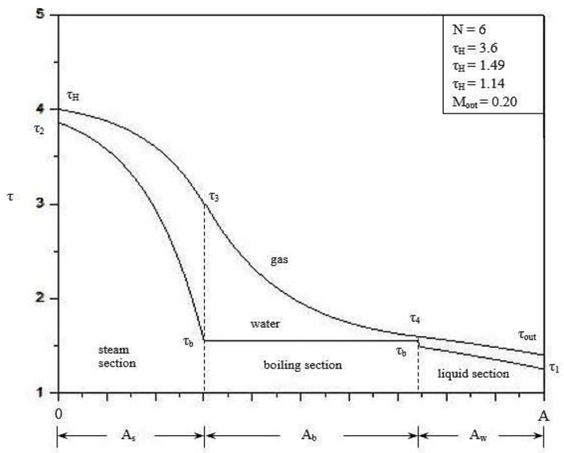

(b)

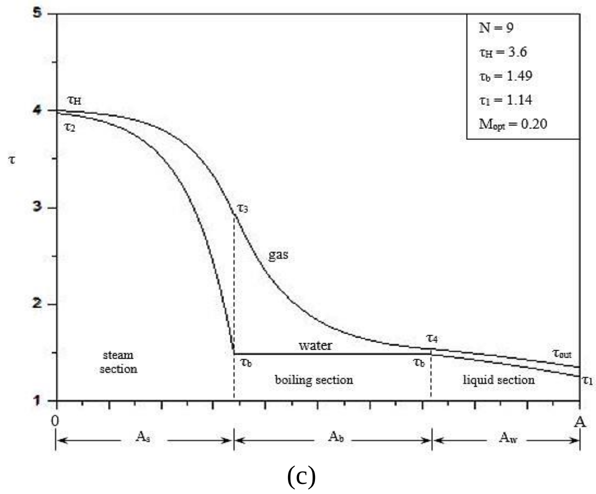

(c)

Figure 3 a – c. The effect of the heat transfer area size on the temperature distributions of the two streams.

In Figure 3, it is observed that as the size of the heat exchanger (N) increases, the temperatures of both streams become narrower. The temperature and area distribution of Fig. 3 is represented by adopting a fixed mass flow as determined by the following expression:

$$M = \frac{\dot{m}_w}{\dot{m}} = \mu \frac{c_p}{\bar{c}_s} \tag{43}$$

We found that if we vary M the temperature distributions shift, and second law efficiency exhibits a maximum at a certain value, M_{opt}. The optimum thermodynamic occurs when all three sections are present. This effect is observed in Figure 4, where it is shown that the model adopted for the respective vapor properties has a marked effect on the optimum, being determined that M_{opt}=0.18. The numerical results analyzed are based on the tabulated properties of the vapor according to (Moran et al., 2011). Note that each frame in Figure 3 was drawn for the value of M, which maximizes the efficiency of the second law when N, τ_H, τ_b and τ_1 are fixed. After performing the simulation, it was observed that the sections of liquid water and biphasic flow increase as M increases, when M exceeds 0.301, the vapor section disappears completely.

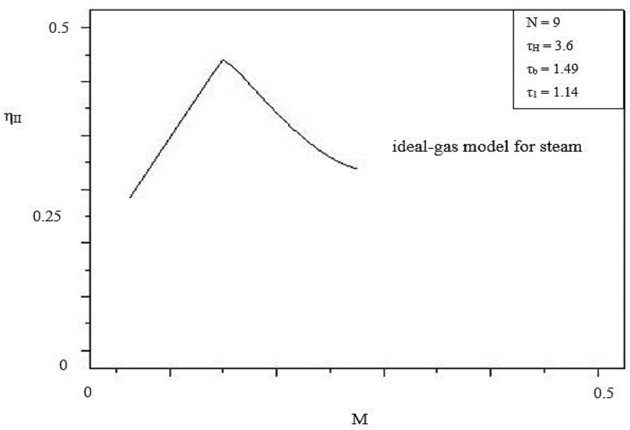

Figure 4. Maximum thermodynamic performance for the *M*.

If optimal thermodynamic existence - optimal ratio M. It means that any current can be optimally matched to another current, such that most of the exergy carried by the hot stream is captured by the cold stream. Another observation the optimal thermodynamic performance is practically insensitive to changes in N when N is greater than five.

5. CONCLUSIONS

The main conclusion is that the extraction of energy from a hot flow can be maximized by the ratio of the hot flow to a cold-water flow through a small fixed size thermal transfer area. The optimal thermodynamic can be located based on the minimization of the total rate of entropy generation subject to the limit rate. When the cold current evaporates by capturing a portion of the exergy of the hot stream, its side of the heat exchanger is divided into three sections: preheating of liquid, boiling and superheating of steam (e.g., figure 3). These sections conform to their appropriate sizes when the system is close to the overall thermodynamic optimum. In the present method, the pressure was not taken into account for the sake of simplicity.

The maximization of the exergy extraction of the hot stream was the objective. We show results for $M < 0.5$ because for our case the optimal ones are in this range. Other applications may require searches across broader ranges of capacity flow ratios.

This optimization principle can be used widely in the conceptual design of power and refrigeration systems. We analyzed the optimal match between two streams, where the colder one undergoes a phase change. This is the case in most power plant design, e.g., Rankine cycle designs. The fundamental problem addressed in this paper is also relevant to designs that are more complex, such as cogeneration systems.

Nomenclature

a, b	thermophysical properties
A	area, m^2
c_s	specific heat of steam at constant pressure, Jkg^{-1} K^{-1}
c_p	specific heat of hot gas at constant pressure,Jkg^{-1}K^{-1}
c_w	specific heat of liquid water, Jkg^{-1} K^{-1}
$\bar{c}_s$	average specific heat of stream at constant pressure.
e_x	specific flow exergy, J kg
h_{fg}	specific latent heat, J kg^{-1}
$\dot{m}$	mass flow rate of hot gas, kg s^{-1}
$\dot{m}_w$	mass flow rate of cold stream, kg s^{-1}
M	ratio of mass flow rates
N	number of heat transfer units
Q_0	rate of heat rejection to the ambient, W
s	specific entropy, J kg^{-1} K^{-1}
$\dot{S}_{gen}$	entropy generation rate, W K^{-1}
T	temperature, K
T_0	ambient temperature, K
U	overall heat transfer coefficient, W m^{-2} K^{-1}
$\dot{W}$	power, W
x, y	area fractions

Greek symbols

ϵ	heat exchanger effectiveness
η_{II}	second law efficiency
μ	ratio of capacity rates
τ	dimensionless temperature, T/T_0

Subscripts

b	boiling section
f	saturate liquid
g	saturate vapor
H	hot stream intel
out	hot stream outlet
s	superheated steam
w	liquid stream

6. ACKNOWLEDGEMENTS

The authors acknowledge for the help presented to the NPDEAS (Nucleus of Sustainable Energy Research and Development) laboratory, allowing them to use their infrastructures to perform tests in the heat exchanger. We recognize the CNPq (National Research Research) for the financial support in the project 403560/2013-6. CEED (Center for Energy Studies for Development) for the economic support that allows me to carry out these investigations.

7. REFERENCES

Albores, P., Petridis, K. and Dey, P.K., 2016. *Analyzing efficiency of Waste to Energy Systems: Using Data Envelopment Analysis in Municipal Solid Waste Management*. International Conference on Solid Waste Management, v. 35, 265-278.

Beede, D. N., and Bloom, D. E., 1995. *The economics of municipal solid waste*. The World Bank Research Observer, v.10, 113-150.

Bejan, A., 1993. *Heat Transfer*, Wiley, New York, Ch. 9.

Bejan, A., 1996. *Entropy generation minimization: The new thermodynamics of finite-size devices and finite-time processes*. Journal of Applied Physics, v. 79, 1191-1214.

Bejan, A., Errera, R., 1998. *Maximum power from a hot stream*. International journal heat mass transfer, v. 41, 2025-2036.

Bejan, A., 1996. Entropy Generation Minimization, CRC Press.

Bruel, C., Chiron, F.X., Tavares, J.R., Patience, G.S., 2016. *An exponential expression for gas heat capacity, enthalpy, and entropy*. Experimental Thermal and Fluid Science, v. 78, 249-253.

Liu, Y., & Liu, Y., 2005. *Novel incineration technology integrated with drying, pyrolysis, gasification, and combustion of MSW and ashes verification*. Environmental science & technology, v.39, 3855-3863.

Lombardi, L., Carnevale, E., Corti, A., 2015. *A review of technologies and performances of thermal treatment systems for energy recovery from waste*. Waste Management, v. 37, 26-44.

Manjunath, K., Kaushik, S.C., 2014. *Second law thermodynamic study of heat exchangers: A review*. Renewable and Sustainable Energy Reviews, v.40, 348-374.

Moran, J. M., Shapiro, H.N., Boettner, D.D. and Bailey, M.B., 2011. *Fundamentals of Engineering Thermodynamics.* 7th edition. Wiley & Sons, Ch. 6, 7 and 8.

Vargas, J.V.C and Araki, L. K., 2016. *Applied numerical calculation*. First edition. Manole.

Vargas, J.V.C, Fleming, J.S., Parise, J.A.R., 2001. *Maximum exergy input rate from a hot stream in solar-driven refrigerators*. International journal of energy research, v.25, 751-767.

8. RESPONSIBILITY NOTICE

The authors are the only responsible for the printed material included in this paper.